



# Chemical modification of chitosan with cationic hyperbranched dendritic polyamidoamine and its antimicrobial activity on cotton fabric

Benjamas Klaykrueyat<sup>a</sup>, Krisana Siralermukul<sup>b</sup>, Kawee Srikulkit<sup>a,c,\*</sup>

<sup>a</sup> Department of Materials Science, Faculty of Science, Chulalongkorn University, Bangkok 10330, Thailand

<sup>b</sup> Metallurgy and Materials Science Research Institute, Chulalongkorn University, Bangkok 10330, Thailand

<sup>c</sup> National Center of Excellence for Petroleum, Petrochemicals and Advanced Materials, Bangkok 10330, Thailand

## ARTICLE INFO

### Article history:

Received 25 September 2009

Received in revised form 4 November 2009

Accepted 9 November 2009

Available online 13 November 2009

### Keywords:

Cationic hyperbranched polyamidoamine

Modification of chitosan

Antimicrobial activity

*S. aureus*

Cotton fabric

## ABSTRACT

The cationic hyperbranched dendritic polyamidoamine (PAMAM) containing terminal methyl ester end groups was synthesized and then employed for modifying flake chitosan. The synthesis was achieved using repetitive reactions between Michael addition and amidation to obtain the methyl ester group terminated hyperbranched PAMAM, and then the methyl ester terminated hyperbranched dendritic PAMAM (PAMAM-ester) was methylated with dimethyl sulphate. The subsequent modification of chitosan with the cationic hyperbranched PAMAM-ester was carried out at room temperature for 5 days. As a result, cationic hyperbranched PAMAM modified chitosan was achieved. Characterizations by elemental analysis, FT-IR, NMR, TGA and XRD were employed to investigate the structural changes of chitosan to confirm its configuration. The cationic hyperbranched PAMAM-chitosan was applied onto cotton fabric at 1 wt.% add-on using a padding method and was found to have a good antimicrobial performance against *Staphylococcus aureus* compared to that obtained with unmodified chitosan.

© 2009 Elsevier Ltd. All rights reserved.

## 1. Introduction

Chitosan, a deacetylated derivative of chitin, is a natural, low-toxic, biodegradable polymer that is resistant to microbial growth. The antimicrobial activity of chitosan is well known and involves the polycationic nature of chitosan which is capable of binding with anionic sites in microbe's proteins. However, its cationic nature is governed by pH, only being the case at acidic conditions (<pH 6) and this limits the range or performance of chitosan application. In addition, the chitosan-mediated inhibition of bacterial and fungal growth depends on the molecular weight and functional groups of chitosan. When compared to high Mw chitosan, oligomeric chitosan can penetrate the cell membrane of a microorganism and prevent the growth of the cell by inhibiting RNA transcription. From an applicability point of view, as well as its antimicrobial capability, chitosan's limited solubility in water to within the acidic range only is important and limiting. To overcome this, chitosan derivatives that are soluble in water over a wide pH range have been prepared by introducing a quaternary ammonium group or a polymeric quaternary ammonium moiety into chitosan side chain. Chemical modifications of chitosan by these means have

been used to produce chitosan derivatives, such as *N*-[(2-hydroxy-3-trimethylammonium)propyl]chitosan chloride, which exhibits an enhanced antimicrobial activity (Lim & Hudson, 2004), or polyethyleneimine grafted chitosan (Kim et al., 2007) and trimethylated chitosan (Kean, Roth, & Thanou, 2005) which show an improved transfection efficiency. Recently, hyperbranched polyamidoamine (PAMAM), a dendrimer analogue that is a starburst polymer with a plurality of terminal functional groups, has attracted considerable interest due to its novel functionalities, such as nanoscopic containers (SayedSweet, Hedstrand, Spider, & Tomalia, 1997), gene therapy (Majoros, Williams, & Baker, 2008) and ultrafine colloid stabilizer (Marty, Martinez-Aripe, Mingotaud, & Mingotaud, 2008). Modification of terminal groups with different functionalities, such as acetamid, hydroxyl, carboxyl or quaternary ammonium, further leads to the versatile applicability of these materials (Vogtle, Gestermann, Hesse, Schwierz, & Windisch, 2000). For example, quaternized PAMAM dendrimers have a potent antimicrobial activity (Chen et al., 2000). In another aspect, 'dendrimer-like' hyperbranched polyamidoamine can be incorporated into silica (Punyacharoenon & Srikulkit, 2008) or chitosan powder surface (Tsubokawa & Takayama, 2000), resulting in hybrid materials with versatile functionalities.

In this work, the grafting of cationic hyperbranched dendritic PAMAM onto chitosan was investigated with the aim to prepare a modified chitosan with a good water solubility and high antimicrobial activity over a wide pH range. Firstly, hyperbranched

\* Corresponding author. Address: Department of Materials Science, Faculty of Science, Chulalongkorn University, Bangkok 10330, Thailand. Tel.: +66 22185543; fax: +66 22185561.

E-mail addresses: [kawee@sc.chula.ac.th](mailto:kawee@sc.chula.ac.th), [kawee.s@chula.ac.th](mailto:kawee.s@chula.ac.th) (K. Srikulkit).

dendritic PAMAM was synthesized according to Tomalia's well-known method by repetitive reactions between Michael addition and amidation (Tomalia et al., 1985). In this study, synthesis of hyperbranched dendritic PAMAM up to generation 2.5 was targeted. Quaternization of the methyl ester terminated hyperbranched dendritic PAMAM was then carried out by methylation with dimethyl sulphate leading to the production of a cationic hyperbranched dendritic PAMAM-ester, which was employed for modifying flake chitosan. The putative structure of cationic hyperbranched PAMAM-chitosan was proposed as shown in Fig. 1. Characterizations, including elemental analysis, FT-IR,  $^1\text{H}$  NMR, XRD and TGA were employed to investigate the change in the chitosan structure and its properties. The cationic hyperbranched dendritic PAMAM-chitosan was applied onto cotton fabric and its antimicrobial efficiency was preliminarily evaluated against *Staphylococcus aureus* as films and on cotton fabric to compare with that for chitosan.

## 2. Experimental

### 2.1. Materials

Commercial-grade chitosan flake (approx. 85% degree of deacetylation) with a molecular weight of about  $10^6$  Da was purchased from Ebase Co., Ltd. ethylene diamine (EDA) and methyl acrylate (MA) were purchased from Fluka (Switzerland). Commercial-grade methanol was purchased from TSL Chemical (Thailand) Co., Ltd. and distilled prior to use. Dimethyl sulphate (commercial grade) was kindly provided by Modern Dyestuff & Pigment Co., Ltd., (Thailand). Glacial acetic acid was purchased from Merck Chemicals Ltd. Bleached plain woven cotton fabric ( $120\text{ g/m}^2$ ) was purchased from Bigger Text Co., Ltd, Thailand, and used as received.

### 2.2. Synthesis of hyperbranched dendritic PAMAM

The Michael addition step was carried out as follows: a solution of EDA (50 g, 0.833 mol) in methanol (200 ml) was added dropwise to a stirred solution of MA (350 g, 4.069 mol) in methanol (200 ml) at  $0^\circ\text{C}$  over a period of 2 h. The mixture temperature was then

allowed to rise to room temperature ( $\sim 25^\circ\text{C}$ ) and the mixture was continuously stirred for 48 h. The solvent and excess MA were then removed using a rotary evaporator under reduced pressure at  $50^\circ\text{C}$  leaving the methyl ester terminated hyperbranched PAMAM (G0.5).

The amidation step was conducted as follows: a solution of first round Michael addition (G0.5) hyperbranched PAMAM (100 g) in methanol (100 ml) was carefully added to a vigorously stirred solution of EDA (60 g, 1 mol or four times higher than that of the methyl ester content) in methanol (300 ml) at  $0^\circ\text{C}$ . The rate of addition was carefully controlled to assure that the temperature did not rise over room temperature. After completion of EDA addition, the mixture was stirred for 72 h at room temperature. The solvent and unreacted EDA were removed under reduced pressure at a temperature of not higher than  $50^\circ\text{C}$ . The excess EDA was removed to completion (indicated by the absence of EDA vapour detected by pH test paper) at azeotropic temperature using a 9:1 (v/v) ratio of toluene to methanol to yield G1.0 hyperbranched PAMAM.

The second round synthesis was then repeated as above, except that a two times higher concentration of MA was used than that in the first round synthesis, to yield the G1.5 and G2.0 products, and then again to yield the G2.5 hyperbranched PAMAM product.

### 2.3. Methylation of methyl ester terminated hyperbranched dendritic polyamidoamine (PAMAM-ester)

To a solution of G2.5 hyperbranched PAMAM-ester (20 g, 0.007 mol) in methanol (200 ml) with pH value of 9.5–10, 13 g (0.1 mol) of dimethyl sulphate was slowly added. The methylation reaction proceeded immediately at room temperature. The otherwise gradual decrease in the pH was controlled by the addition of concentrated sodium hydroxide solution in order to drive the reaction forward. The pH value of the mixture was maintained at 7.0. The mixture temperature was controlled at room temperature ( $\sim 25^\circ\text{C}$ ) and continuously stirred. After completion of the dimethyl sulphate addition, the mixture was stirred for an additional 30 min to yield the resultant cationic hyperbranched PAMAM-es-

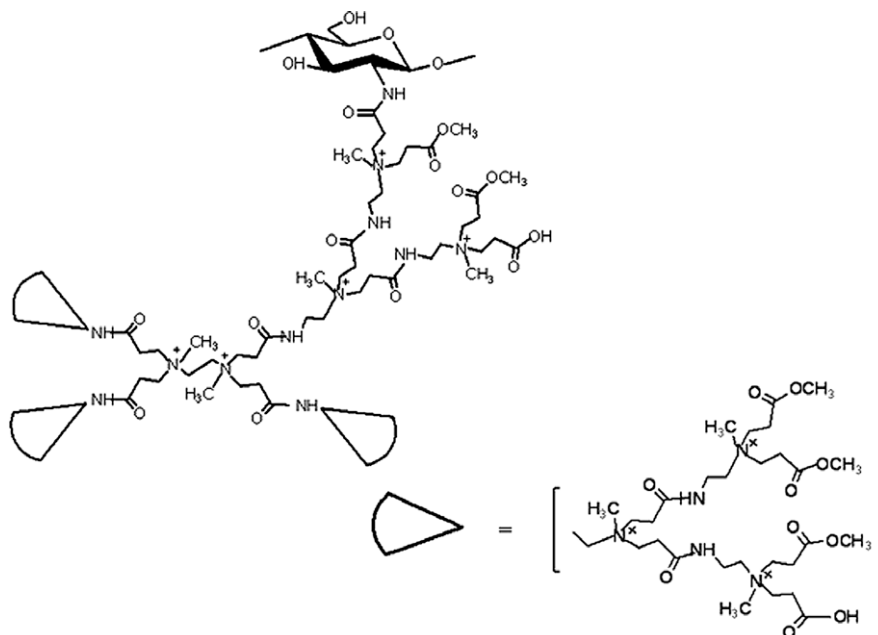


Fig. 1. The putative structure of the G2.5 cationic hyperbranched PAMAM-chitosan.

ter, which was subsequently employed in the next step without purification.

#### 2.4. Modification of chitosan with cationic hyperbranched dendritic polyamidoamine-ester

The modification of chitosan with varying amounts of cationic hyperbranched PAMAM-ester was carried out as follows: a mixture of 5 g chitosan and one of three amounts of G2.5 cationic hyperbranched PAMAM-ester (10%, 50% (w/w) based on chitosan and a five times higher amount of chitosan, the latter represented the excess amount (25 g of liquid cationic PAMAM) in which 5 g chitosan powder was directly dispersed) were dissolved in 50 ml of 1% (v/v) acetic acid solution and stirred by a magnetic stirrer at about 700 rpm until the dissolution was complete (in case of 10 wt.% and 50 wt.%). The solution's pH was then carefully adjusted to pH 7.5 using dilute NaOH solution. The resultant slurry mixture was continuously stirred at room temperature for 5 days to achieve the reaction between the free amine group of chitosan and the methyl ester group of the PAMAM-methyl ester. In the cases of the addition of 10% and 50% (w/w) PAMAM, the solid suspension obtained was filtered and the filtrate then washed thoroughly with distilled water. The obtained wet cake was kept in a desiccator prior to characterization. In the case of excess PAMAM, the obtained viscous liquid was first precipitated in methanol prior to filtration and then washing as above. These three PAMAM-chitosan conjugates are referred to simply as 10%, 50% and excess PAMAM-chitosan from hereon.

#### 2.5. Antimicrobial activity of chitosan and cationic hyperbranched pamam-chitosan applied onto cotton fabric or as films

Chitosan coating solutions (10 g/l) in 1% (w/v) aqueous acetic acid and G2.5 cationic hyperbranched PAMAM-chitosan aqueous solutions (10 g/l and 40 g/l) were prepared. In this study, only the excessively modified (i.e. derived from synthesis with an excess PAMAM) cationic hyperbranched PAMAM-chitosan was selected. For film casting, the prepared solutions were poured into a petri dish and allowed to dry freely at room temperature. Cotton fabrics (8.5 g, size 25 × 28 cm) were padded with prepared chitosan solutions using a Labtec padding machine to provide 100% wet pick up (resulting in 1% wt.% add-on onto the fabric in case of 10 g/l concentration). The padded samples were dried at 100 °C for 10 min and then cured at 150 °C for 3 min in a Rapid laboratory stenter to fix the chitosan or cationic hyperbranched PAMAM-chitosan onto the cotton fibers. The chitosan-fabric was then further treated with 20 g/l aqueous sodium nitrite (NaNO<sub>2</sub>) at room temperature for 30 min in order to achieve a low Mw chitosan-fabric. This experiment was aimed at comparing antimicrobial activity between high Mw chitosan and low Mw chitosan. The treated fabrics were washed thoroughly in de-ionized water and dried prior to antimicrobial activity evaluation. In case of fabric treated 4 wt.% cationic hyperbranched PAMAM-chitosan, the treated fabric was evaluated for wash fastness property according to AATCC Test Method No. 61–2001. The test was performed using a laundering machine (Gyrowash) at 40 °C for 30 min. The fabric surface characteristics were analyzed using SEM and ATR/FT-IR techniques.

##### 2.5.1. Antimicrobial activity of cationic hyperbranched dendritic PAMAM-chitosan as films

The antimicrobial activity of chitosan and cationic hyperbranched dendritic PAMAM-chitosan film were evaluated by quantitative method. The test was carried out to against *S. aureus* (American Type Culture Collection No. 6538). The microbial reduction was calculated according to the following equation,

$$\text{Reduction (\%)} = \frac{B - A}{B} * 100,$$

where *A* and *B* are the number of bacteria (CFU/ml) from the inoculated treated test samples and blank in the flask incubated for 24 h contact time.

##### 2.5.2. Antimicrobial activity of treated cotton fabrics

The antimicrobial activity of treated cotton fabrics were evaluated by quantitative method according to AATCC Test Method 100–1999 (Antibacterial Finishes on Textile Material). The test was carried out to against *S. aureus* (American Type Culture Collection No. 6538). The microbial reduction was calculated according to the following equation,

$$\text{Reduction (\%)} = \frac{B - A}{B} * 100,$$

where *A* and *B* are the number of bacteria from the inoculated treated test samples in the flask incubated for 24 h contact time and 0 h contact time (immediately after inoculation). Visual detection was recorded at 0 and 24 h contact time using a digital camera.

#### 2.6. Characterizations

CHN analysis was performed on PerkinElmer 2400 series II CHNS/O Analyzer. The infrared (FT-IR) spectra were recorded at the frequency range of 4000–400 cm<sup>−1</sup> with 64 consecutive scans at a 4 cm<sup>−1</sup> resolution on a Nicolet 6700 FT-IR spectrometer. <sup>1</sup>H NMR (300 MHz) spectra were recorded on Bruker DPX-300 spectrometer. Test samples of hyperbranched PAMAM and cationic hyperbranched PAMAM-esters were dissolved in D<sub>2</sub>O, while cationic hyperbranched PAMAM-chitosan was first dissolved in CD<sub>3</sub>COOD prior to <sup>1</sup>H NMR measurement. X-ray diffraction (XRD) was performed using a PW 3710 Philips diffractometer with CuKα radiation (λ = 0.1542 nm) and operated at 40 kV and 30 mA. Thermal gravimetric analysis (TGA) was carried out using a Mettler Toledo Stare System DCS822e Module. The results were acquired with a heating rate of 10 °C/min from 30 to 900 °C under nitrogen gas at constant flow rate of 20 ml/min. The fabric surface characterizations were examined by a scanning electron microscope JEOL Model JSM-5410LV and ATR/FT-IR (Nicolet 6700 FT-IR spectrometer).

### 3. Results and discussion

#### 3.1. Elemental analysis

The results from elemental CHN analysis of the chitosan and 4 modified chitosans (Table 1) revealed that the relative amounts of C and N in the chitosan powder are 40.20 and 7.42 mass%, respectively. The %C and %N found in cationic hyperbranched PAMAM-chitosan are notably lower than chitosan powder whilst the %H of the modified chitosan is found slightly different to that of native chitosan. According to the general appearance, the cationic hyperbranched PAMAM-chitosan is moisture sensitive,

**Table 1**

Relative composition (as % by weight) of hydrogen (H), carbon (C) and nitrogen (N) in chitosan (CTS) and the three PAMAM-chitosan derivatives.

Sample	%C	%H	%N
Chitosan (CTS)	40.20	7.25	7.42
10 wt.% PAMAM-CTS	37.55	7.06	7.03
50 wt.% PAMAM-CTS	19.77	8.04	3.21
Excessive PAMAM-CTS	33.07	7.12	6.10

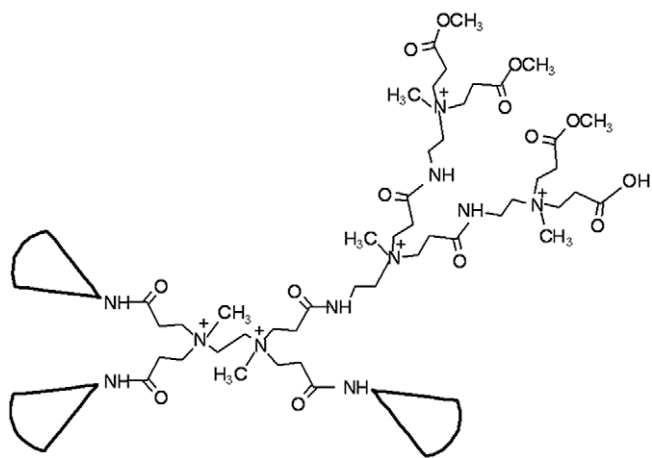


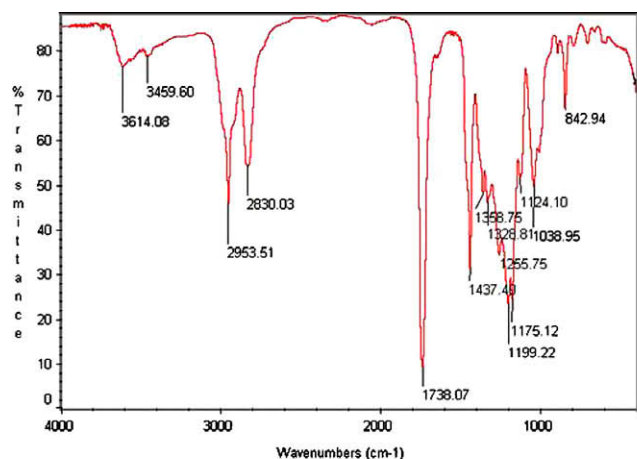
Fig. 2. The putative structure of G2.5 cationic hyperbranched PAMAM.

resulting in existing in wet cake form. This phenomenon is arising from the presence of bound water due to its moisture sensitivity. In case of chitosan modified with an excess amount of cationic hyperbranched PAMAM, the obtained cationic hyperbranched PAMAM-chitosan is water soluble at neutral pH due to the loosely packed

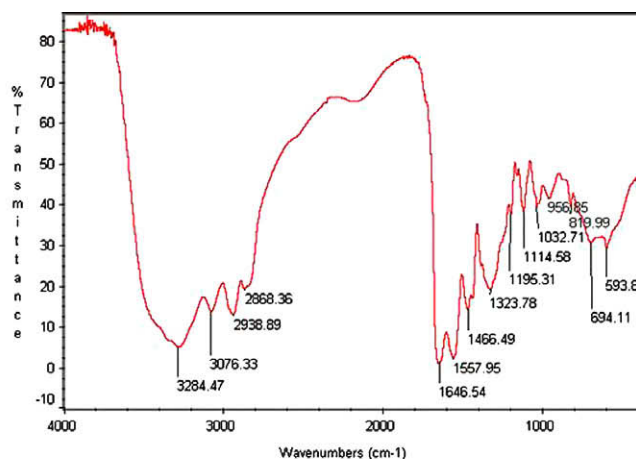
structure and the absence of crosslink. As a matter of fact, the presence of H and O from moisture is associated to the decrease in %C and %N. It was also likely that during the course of methylation reaction the methyl ester terminal groups of the cationic hyperbranched PAMAM could be partially hydrolyzed and converted into the carboxylic acid end groups ( $-\text{COOH}$ ) as proposed in Fig. 2. As a consequence, the decrease in %C and %N were partly associated with the additional OH group content.

### 3.2. FT-IR analysis

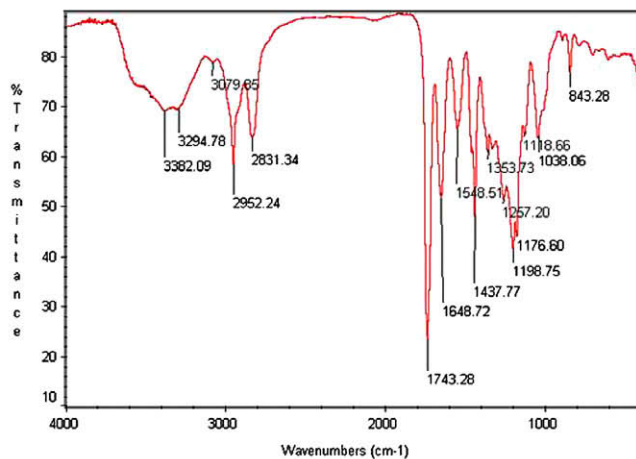
The hyperbranched PAMAM polymers obtained from repeating the (i) Michael addition (G0.5, G1.5 and G2.5 products) and (ii) amidation (G1.0 and G2.0) reactions were characterized using FT-IR analysis. FT-IR results of G0.5, G1.5 products and G1.0 product are shown in Fig. 3. In Michael addition steps, a strong absorption band around  $1740\text{ cm}^{-1}$  is observed, attributed to the methyl ester group. This peak completely disappears in the spectrum of G1.0 as a result of the amidation reaction and the acquired terminal amine group corresponds to the appearance of the strong absorption intensity of the N–H band in the region of  $3000\text{--}3350\text{ cm}^{-1}$ . Indeed, its absorption intensity increases strongly with increasing PAMAM generations, reflecting the fact that the number of terminal amine groups also significantly increases with increasing syn-



(a) G0.5



(b) G1.0



(c) G1.5

### FTIR spectra of hyperbranched PAMAM

Fig. 3. FT-IR spectra of the three different hyperbranched PAMAM from the sequential generations of Michael addition (G0.5) – amidation (G1.0) – Michael addition (G1.5).

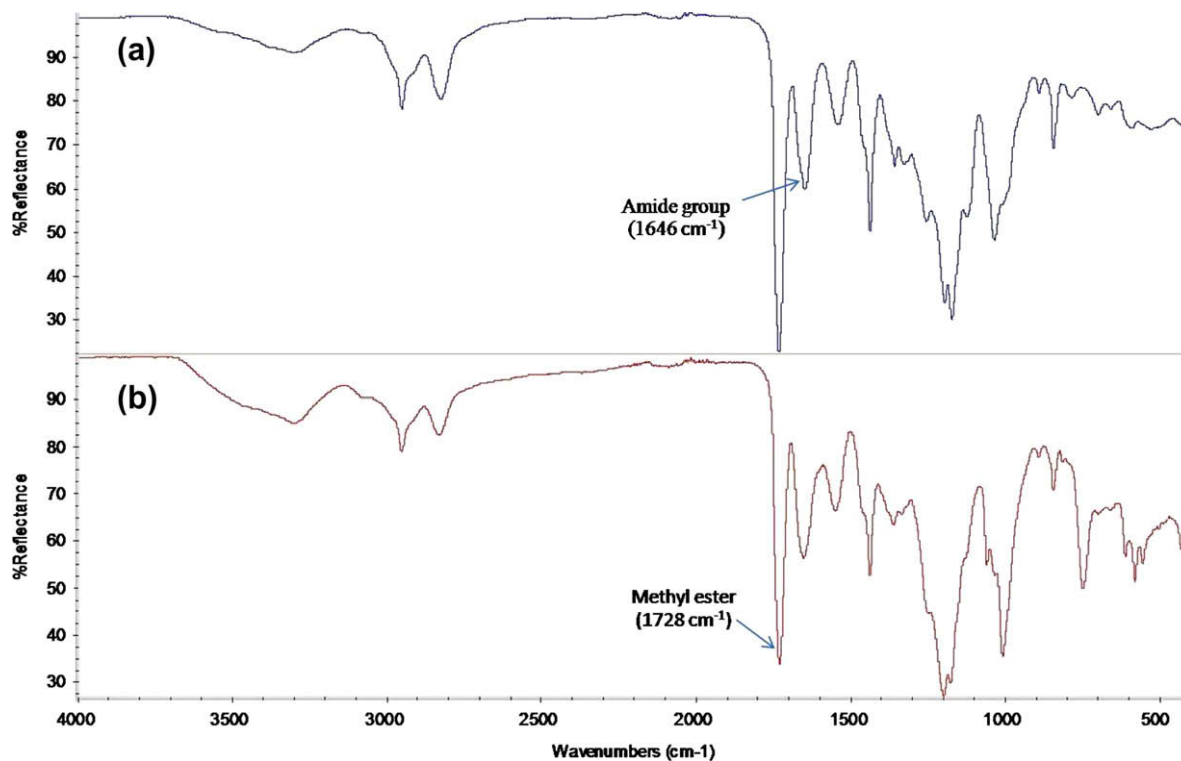


Fig. 4. FT-IR spectra of (a) the G2.5 hyperbranched PAMAM and (b) the G2.5 cationic hyperbranched PAMAM-ester.

thesis rounds. It should be noted that the intensity of amine groups in the spectrum of the G1.5 hyperbranched PAMAM significantly decreases as a result of the Michael addition which converted the amine group of G1.0 PAMAM to a terminal methyl ester group. The FT-IR spectrum for G2.0 is not presented which was found in

similar manner to that shown in the previous report (Punyacharoennon & Srikulkit, 2008).

The FT-IR spectrum of the G2.5 cationic hyperbranched PAMAM-ester is similar to that of the G2.5 hyperbranched PAMAM-ester (Fig. 4). The intensity of the C=O ester vibration

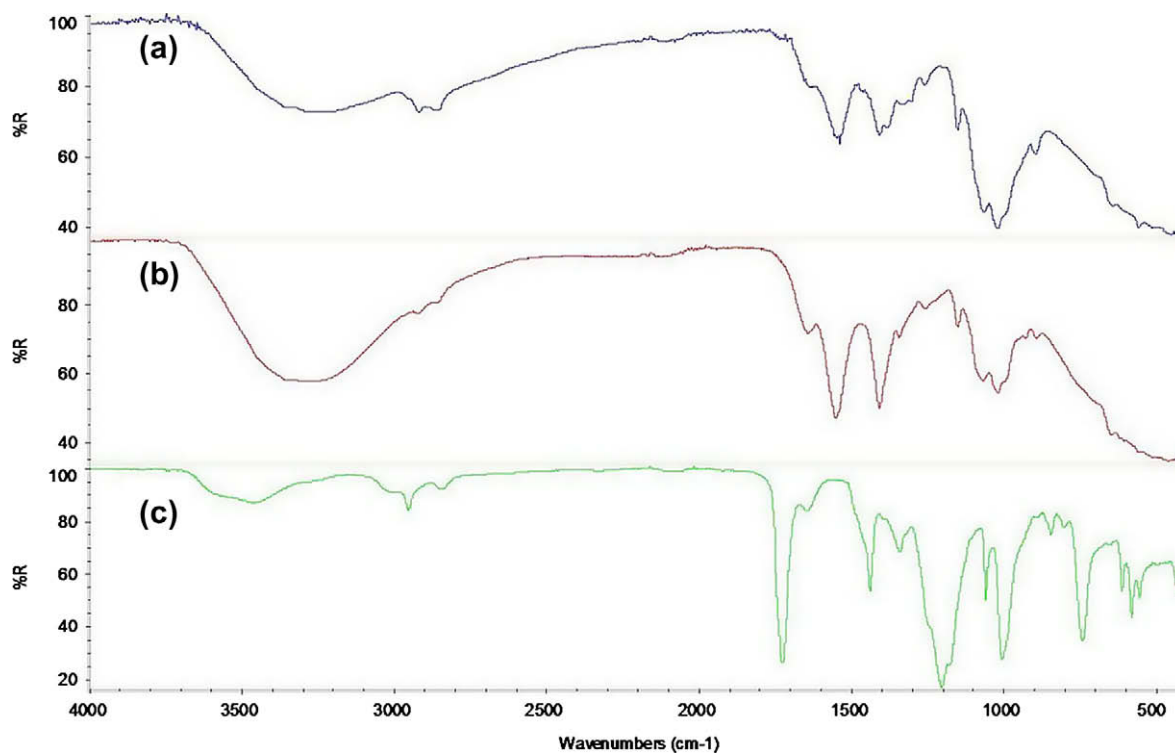


Fig. 5. FT-IR spectra of (a) chitosan; (b) 50 wt.% hyperbranched dendritic PAMAM-chitosan and (c) excessive cationic hyperbranched dendritic PAMAM-chitosan.



(1728  $\text{cm}^{-1}$ ) peak of the cationic hyperbranched PAMAM is slightly less than that of the hyperbranched PAMAM-ester, indicating that a partial loss of some of the C=O ester groups occurs in the methylation step. It is likely that some of the C=O ester groups were hydrolyzed and converted into COOH groups. Indeed, the FT-IR results provide supportive evidence along with the EA analysis to underline that during the quaternization step and the modification of chitosan, the methyl ester group of the cationic hyperbranched PAMAM underwent competitive hydrolysis.

The FT-IR spectrum of the 50% (w/w) cationic hyperbranched dendritic PAMAM-chitosan exhibits an absorption fingerprint that is largely similar to that of native chitosan (Fig. 5), as expected due to their similarity in chemical structure. Despite the spectral similarity, the differences in the intensity between the weaker chitosan amide band and the much stronger PAMAM-chitosan amide band at 1646  $\text{cm}^{-1}$  is noticeable, indicating that the PAMAM-chitosan has a higher content of amide groups than unmodified chitosan. The spectrum derived from the excess PAMAM-chitosan also shows broadly similar trends as the above, but with a strong peak at  $\sim 1720 \text{ cm}^{-1}$  representing methyl ester pendant group. This increase in the amide band intensity arose from the reaction between the chitosan amine group and the PAMAM-methyl ester group, yielding an amide linkage. The presence of methyl ester pendant group in the excess PAMAM-chitosan thanks to the usage of excessive amount of cationic hyperbranched PAMAM could act as a reactive group in the application point of view. Based on these evidences, the putative structure of the G2.5 cationic hyperbranched PAMAM-chitosan, formed with an excess amount of cationic hyperbranched PAMAM, is proposed as shown in Fig. 1.

### 3.3. $^1\text{H}$ NMR analysis

The  $^1\text{H}$  NMR spectrum of the G0.5 ester terminated PAMAM indicates the presence of the terminal methyl ester group ( $\text{CH}_3\text{—O—}$ ) at  $\sim 3.8$  ppm (Fig. 6), corresponding to the methyl proton of the methyl ester group. In this spectrum, the amide proton signal is absent, indicating that the reaction of EDA with the methyl ester end group could be prevented due to the presence of the excessive amount of methanol, a suppressor of amidation reactions. The methyl ester signal completely disappears from the  $^1\text{H}$  NMR spectrum of G1.0 due to the amidation reaction which resulted in the replacement of the methyl ester group by ethylene diamine. As a result, the amide bond was formed, as confirmed by the appearance of the signal of amide proton at around 7.8 ppm. Thus the synthesis of methyl ester terminated G2.5 hyperbranched PAMAM was achieved, and so was next employed for the preparation of cationic hyperbranched PAMAM-ester.

The  $^1\text{H}$  NMR spectrum of the G2.5 cationic hyperbranched PAMAM-ester reveals the strong presence of the signal associated with the terminal methyl ester group ( $\text{CH}_3\text{—O—C=O}$ ) at  $\sim 3.8$  ppm (Fig. 7), indicating that it was intact during the methylation step. Following the methylation reaction, the methyl group ( $\text{CH}_3\text{—}$ ) was anticipated to be incorporated into the tertiary amine, resulting in a quaternary ammonium moiety being introduced into the hyperbranched PAMAM-ester, as diagrammatically shown in Fig. 2. The signal for the methyl proton should appear at around 3 ppm in vicinity of methylene proton, and, as seen in Fig. 7, it is likely that the strong signal appearing at 3.1 ppm arises from signal overlapping between the methyl and methylene protons.

The  $^1\text{H}$  NMR spectra of chitosan and cationic hyperbranched PAMAM-chitosan reveal the characteristic chemical shifts of chitosan protons at 3.4, 3.2 and 2.6 ppm (Fig. 8), which are assigned to H3–H6 and H2, respectively. For the cationic hyperbranched PAMAM-chitosan, two peak regions were observed between 2.2 and 3.6 ppm, featuring the combination of signals of chitosan protons and hyperbranched PAMAM protons. The

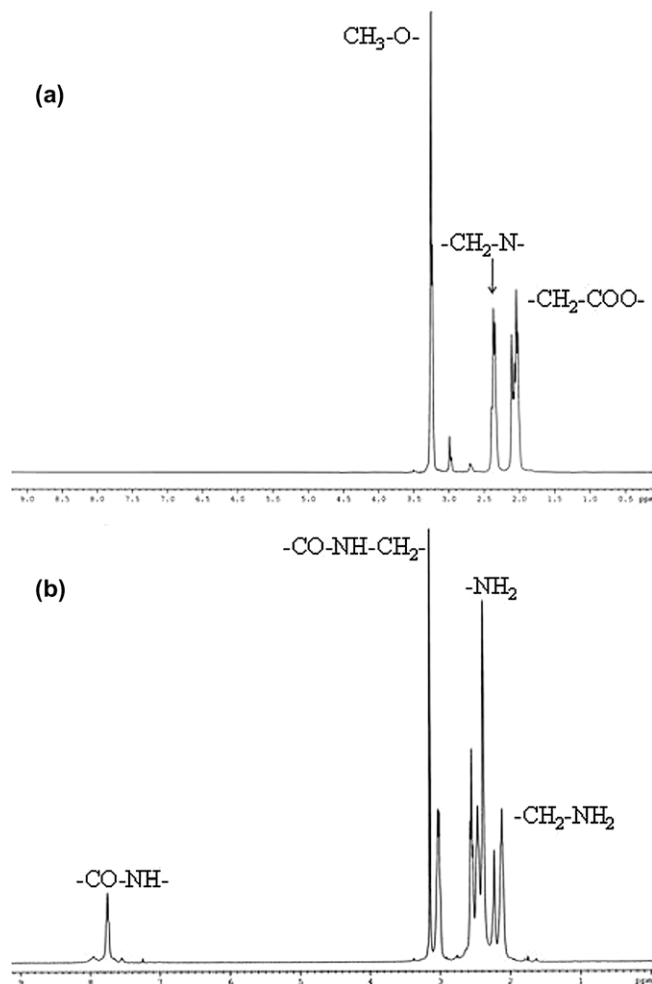


Fig. 6.  $^1\text{H}$  NMR spectra of G0.5 hyperbranched PAMAM (top) and G1.0 hyperbranched PAMAM-ester (bottom).

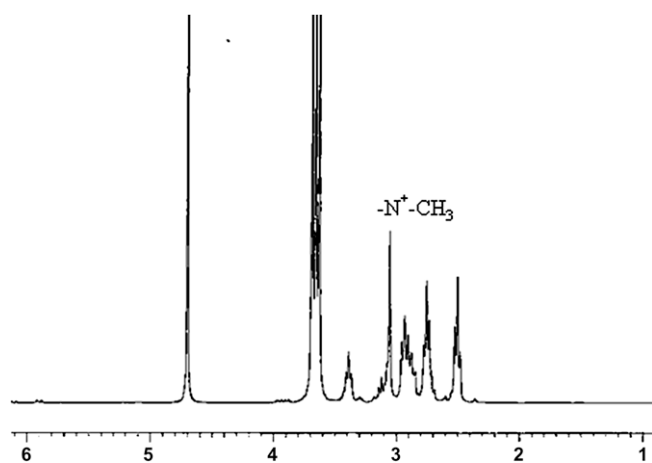


Fig. 7.  $^1\text{H}$  NMR spectrum of G2.5 cationic hyperbranched PAMAM-ester.

signal at 3.1 ppm shows up strongly, presumably due to being the combination of chitosan and PAMAM protons. The signal of the methyl ester proton at 3.8 ppm totally disappears from the spectra of cationic hyperbranched PAMAM-chitosan, indicating that this group easily underwent reactions including, in this system, amidation with chitosan free amine group and hydrolysis (a side reaction).

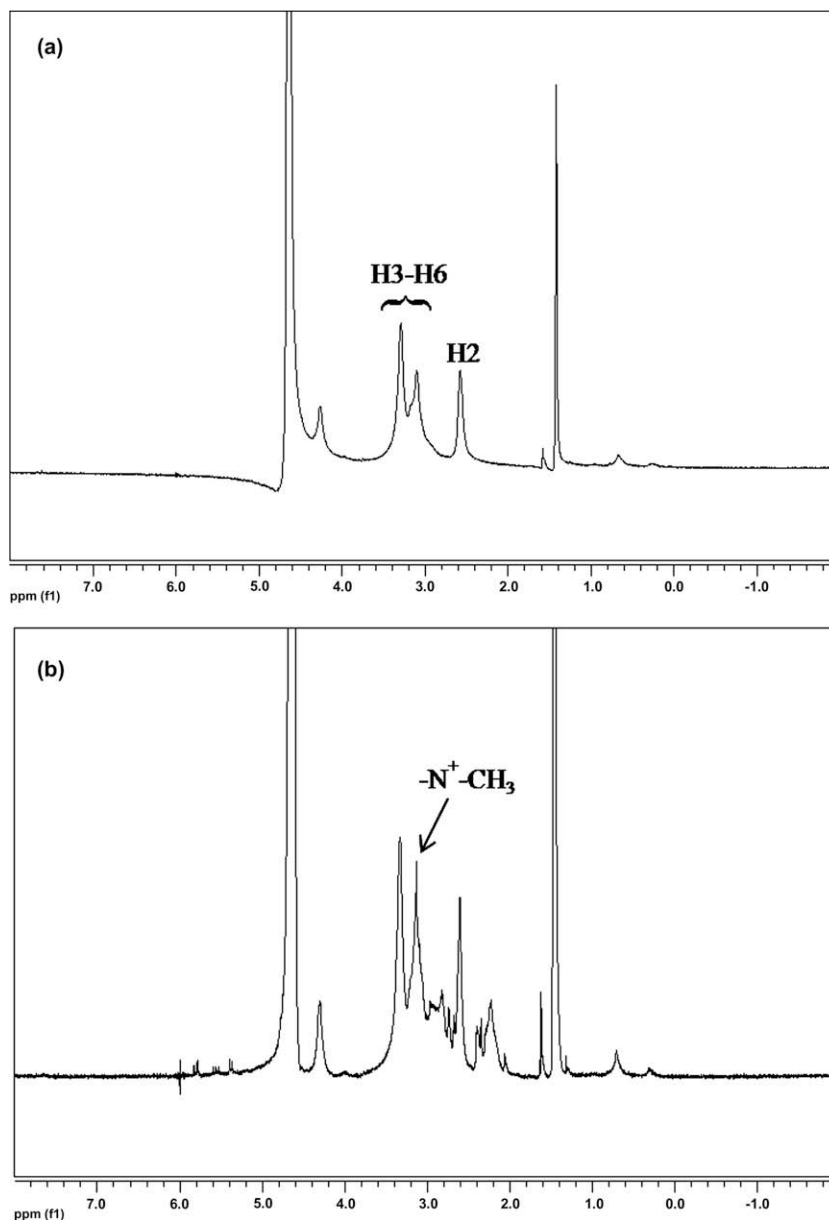


Fig. 8.  $^1\text{H}$  NMR spectra of chitosan and 2.5 cationic hyperbranched PAMAM-chitosan.

### 3.4. TGA analysis of cationic hyperbranched dendritic PAMAM-chitosan

The TGA thermograms of chitosan, cationic hyperbranched PAMAM and cationic hyperbranched PAMAM-chitosans show that chitosan starts to decompose at temperatures above  $200^\circ\text{C}$  with a decomposition peak temperature ( $T_d$ ) of  $307^\circ\text{C}$  (Fig. 9). In contrast, the cationic hyperbranched PAMAM decomposes more easily at  $120^\circ\text{C}$  with  $T_d$  values of  $189$  and  $298^\circ\text{C}$ . For the cationic hyperbranched PAMAM-chitosan, the mass loss occurs in multiple steps within the temperature range of  $100$ – $300^\circ\text{C}$ . Upon initial heating, the gradual loss of mass proceeded with a  $T_d$  of  $126^\circ\text{C}$ , which is probably due to the loss of bound water followed by the degradation of the bonded cationic hyperbranched PAMAM moiety. Further heating resulted in the loss of the chitosan backbone with a decomposition peak temperature of  $287^\circ\text{C}$ . Thus, the  $T_d$  of cationic hyperbranched PAMAM-chitosan is lower when compared to pristine chitosan, indicating the lower thermal stability of the modified chitosan. Since the presence of the bulky cationic hyperbranched

PAMAM group interferes with the close packing between chitosan molecules, it leads to an increase in the polymer chain mobility and chain scission.

### 3.5. X-ray diffraction (XRD)

The XRD diffractograms of film samples including free chitosan and the three different cationic hyperbranched PAMAM-chitosan films are shown in Fig. 10. The broad peak found in the region of  $2\theta = 15^\circ$  to  $30^\circ$  represents the semicrystalline characteristic of a typical chitosan film and indicates that the prepared film exhibits a low crystallinity. Chitosans modified with 10 wt.%, 50 wt.%, and excessive cationic hyperbranched PAMAM was also cast into film for XRD analysis. From Fig. 10, the modified films containing 10 wt.% and 50 wt.% cationic hyperbranched PAMAM exhibit a similar XRD pattern to those of free chitosan, but as the amount of cationic hyperbranched PAMAM was increased so the intensity of the  $2\theta = 15^\circ$  to  $30^\circ$  peak was reduced until, at excessive cationic hyperbranched PAMAM levels, the resultant modified film was

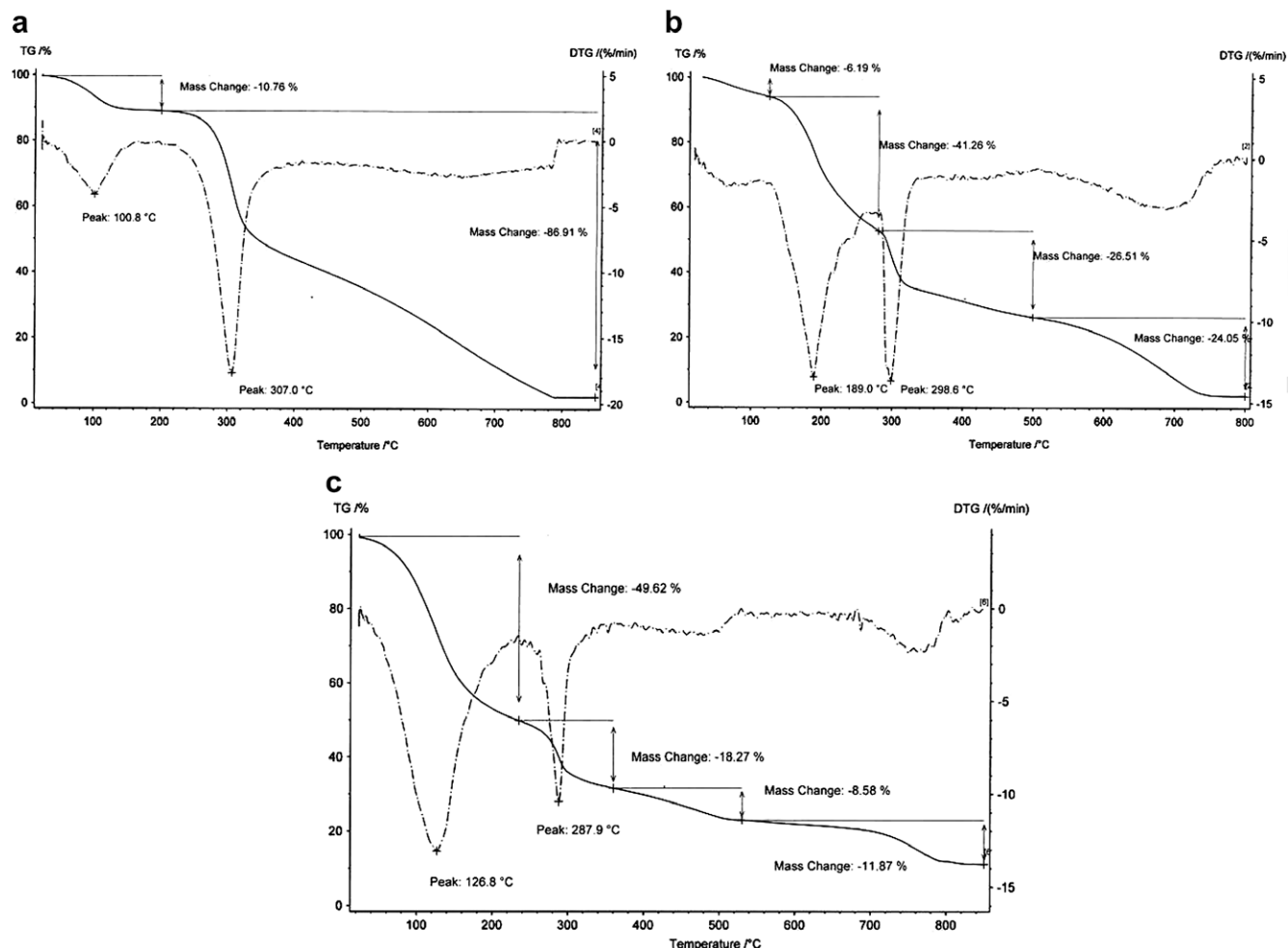


Fig. 9. TGA thermograms of (a) chitosan, (b) 2.5 cationic hyperbranched PAMAM and (c) 2.5 cationic hyperbranched PAMAM-chitosan.

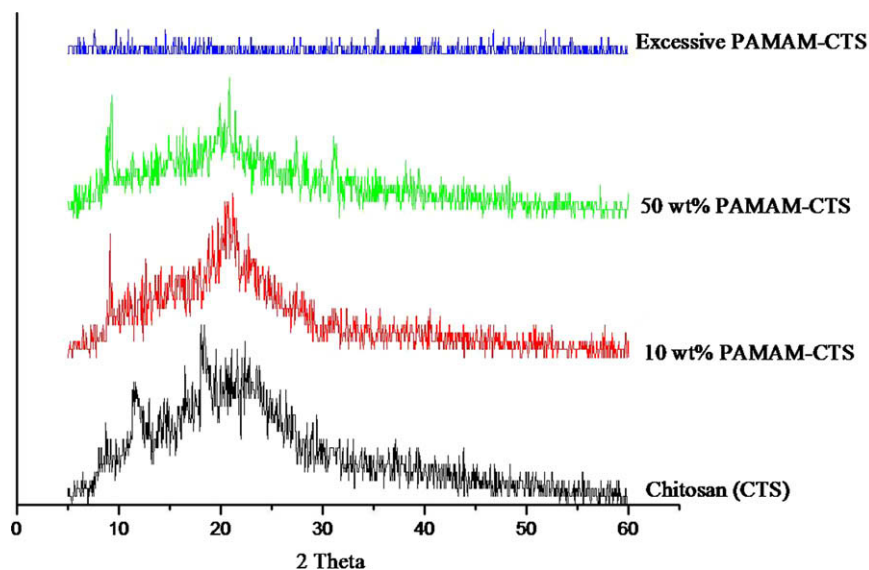


Fig. 10. XRD diffractograms of chitosan and the three different PAMAM-chitosan derivative film samples.

completely amorphous to X-ray diffraction. This phenomenon can be attributed to the fact that the increase in the bulk cationic hyperbranched PAMAM group in the chitosan leads to an increase

in the steric hindrance which directly interferes with the crystallization process of chitosan. As a consequence, the chitosan film containing excessive cationic hyperbranched PAMAM is amor-



phous, as evidenced by the total disappearance of the semicrystalline peak.

### 3.6. Antimicrobial evaluation

The antimicrobial activity of chitosan, and that of cationic hyperbranched PAMAM-chitosan (synthesized with an excess of PAMAM to chitosan), was preliminarily evaluated against *S. aureus* in terms of visual detection and percent microbial reduction using a single application dose (Table 2). A high percentage reduction of bacterial colony indicates a good antimicrobial activity of a sample.



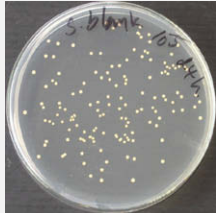







The cotton fabric was coated with flake chitosan (1 wt.% add-on) and then treated with 20 g/l  $\text{NaNO}_2$  for 30 min in order to obtain low Mw chitosan-coated fabric (Srisuk & Srikulkit, 2008). The chitosan-impregnated fabric and resultant low Mw chitosan-impregnated fabric both showed no antimicrobial activity. These indicate that chitosan itself was not sufficient to inhibit the growth of *S. aureus*. However, in a separate experiment, native chitosan film was prepared by film casting and subject to microbial activity test. The result shows that native chitosan film exhibited excellent

antimicrobial activity, which is in contrast to the observed results from chitosan-coated fabrics (Table 2). In this preliminary study any dose effects were not evaluated. It should also be pointed out that the chitosan film used in the antimicrobial test was not neutralized whereas that of the impregnated cotton was. Thus, the native chitosan film was likely to mainly be positively charged amine  $\text{NH}_3^+$  groups, resulting in their excellent antimicrobial activity against *S. aureus*. In contrast, the amino groups of the chitosan on the chitosan-fabric would mainly be present in an uncharged format as a result of the treatment process and, as a consequence, the chitosan-coated fabric exhibited a poor antimicrobial activity. It is true to say that chitosan by nature possesses a mild antimicrobial characteristic which is resistant to microbial growth but not powerful enough to play an antimicrobial role in cotton cellulose which contains plentiful nutrients for microbial growth.

The cationic hyperbranched dendritic PAMAM-chitosan film also exhibited a strong antimicrobial activity against *S. aureus*, which was comparable to that of the native chitosan film. Whether this is also due to its cationic character remains to be evaluated

**Table 2**

Antimicrobial evaluation of chitosan (CTS) and G2.5 cationic hyperbranched PAMAM-chitosan, either as films or after impregnation into cotton fabric, against *S. aureus*.

Sample	wt.% add-on (on fabric)	Visual detection (experimental Section 2.5)		%Reduction
		A	B	
CTS film without neutralization (0.33 g)	–			100
Cat. PAMAM-CTS film (0.25 g)	–			99.99
CTS-fabric	1			0
$\text{NaNO}_2$ depolymerized CTS-fabric	1			0
Cat. PAMAM-CTS-fabric	1			98.75

but, importantly, in contrast to chitosan, cotton fabric treated with cationic hyperbranched dendritic PAMAM-chitosan (1% (w/w)) exhibited excellent antimicrobial activity against *S. aureus*, albeit at a relatively lower level than pure chitosan and cationic PAMAM-chitosan. Thus cationic hyperbranched dendritic PAMAM could potentially enhance the antimicrobial performance of chitosan, and this may be attributable to its cationic character although both these interesting preliminary findings require further characterization and verification. That is, in this preliminary study the potential antimicrobial activity in treated cotton fabrics was only evaluated on one microbial species (*S. aureus*) and one fabric dose (1 wt.% add-on) without subsequent multiple washes. It thus remains essential to evaluate the dose dependence of this effect within the fabric, including its relative resistance to multiple wash cycles of the fabric, as well as the range of applicable microbes that are susceptible under these conditions before firm conclusions can be drawn.

### 3.7. Evaluations of fabric surface characteristics

The fastness property of the cationic chitosan on cotton fabric was evaluated using washing standard test. Fabric samples were subjected to repeated washings up to five cycles. The fiber surface morphology, when analyzed by SEM, was similar to native cellulose surface for 1 wt.% cationic chitosan-fabric and rough for 4 wt.% cationic chitosan-fabrics both before and after five washes (Fig. 11). In case of 1 wt.% cationic chitosan, the presence of chitosan is not observed by SEM analysis due to the low amount of chitosan. Taking the rough surface morphology to represent the presence of cationic chitosan on the fiber surface, the remaining rough surface after five wash cycles suggests the fastness property of cationic chitosan on the cotton surface. However, to confirm the actual existence of cationic chitosan, the same samples were also analyzed by ATR/FT-IR spectroscopy, with representative spectra shown in Fig. 12. It should be noted that the IR spectrum of 1 wt.% cationic chitosan-fabric exhibited a similar fingerprint to that of native fabric, again, due to an insufficient amount of cationic chitosan on fabric surface. The methyl ester band found at  $1728\text{ cm}^{-1}$  taken before thermal fixation in case of the 4 wt.% cationic chitosan treated fabric is indicative of the presence of the cationic chitosan on the fiber surface. This absorption band remained with a notable intensity after the fabric had been thermofixed at  $150^\circ\text{C}$ . In addition, the amide peak shows up clearly at  $1639\text{ cm}^{-1}$ . However, the ester band completely disappears after the fabric had been repeatedly washed for five cycles, indicating

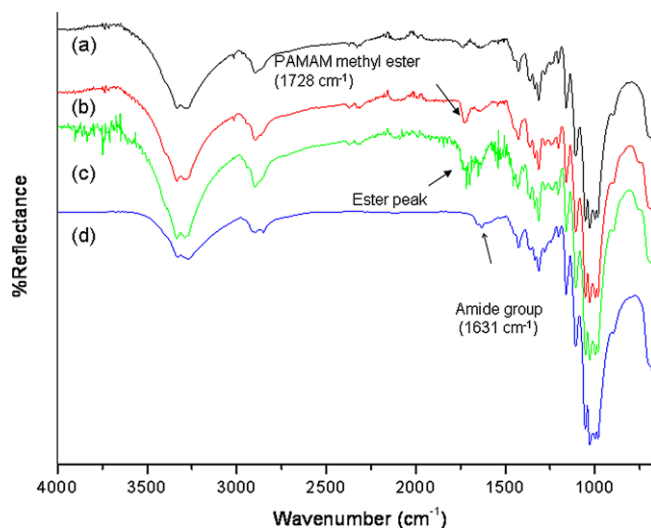


Fig. 12. ATR/FT-IR spectra of (a) cotton fabric, (b) 4 wt.% cationic chitosan cotton fabric before thermofixation, (c) 4 wt.% cationic chitosan cotton fabric after thermofixation, (d) 4 wt.% cationic chitosan cotton fabric after five wash cycles.

the weak hydrolytic stability of an ester bond. On the other hand, the amide bond still exists, indicating the durability of cationic chitosan. It is thought that the adhesion of cationic chitosan on the fabric surface is dependent on the cationic group of chitosan and hydrogen bonding between amide group and cellulose hydroxyl group.

### 4. Conclusions

The incorporation of cationic hyperbranched PAMAM into the chitosan backbone was carried out through a straightforward reaction of the PAMAM-methyl ester end group and the chitosan amine group. The amide linkage was formed, as evidenced by FT-IR analysis. Proton NMR results showed that cationic hyperbranched PAMAM-chitosan exhibited two signal regions that correspond to chitosan and hyperbranched PAMAM protons. Interestingly, chitosan modified with an excess amount of cationic hyperbranched PAMAM-ester remained both water soluble and with potential antimicrobial activity at a neutral pH, in contrast to native chitosan. TGA analysis supported that the cationic hyperbranched PAMAM-chitosan contained water bound and a bulky side group

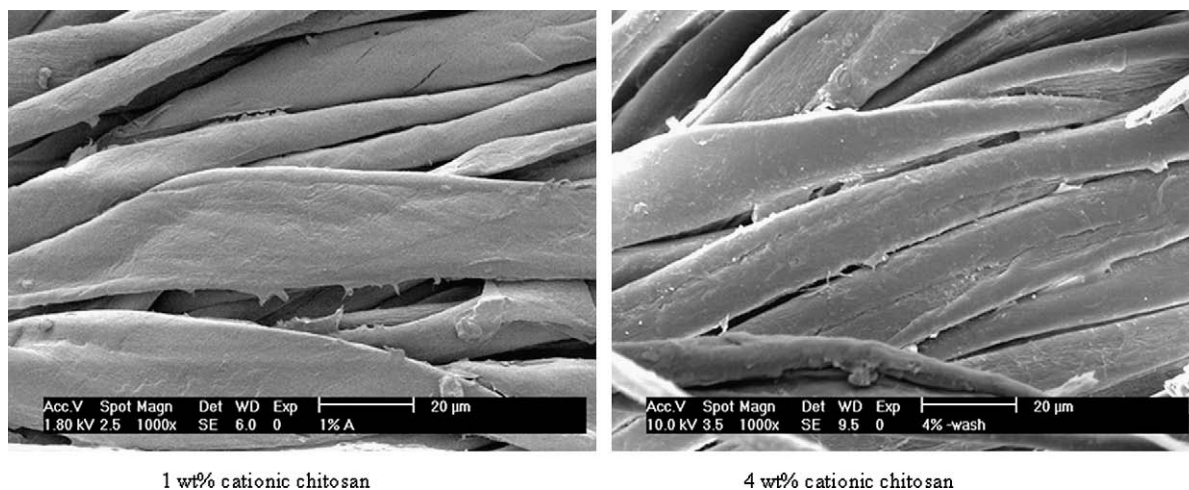


Fig. 11. SEM micrographs of 1 wt.% cationic chitosan cotton fabric and 4 wt.% cationic chitosan cotton fabric taken after five wash cycles.

that interfered with the packing of chitosan molecules. In addition, XRD analysis supported that cationic hyperbranched PAMAM-chitosan exhibited a completely amorphous film, again presumably due to the effects of the steric side group. Based on these results, it is concluded that the presence of the bulky side group enhanced the chain mobility and water solubility of the modified chitosan.

Chitosan modified with cationic hyperbranched PAMAM exhibited an excellent antimicrobial activity against *S. aureus* even at a near neutral pH and when impregnated into cotton fabrics and so potentially could enhance the antimicrobial activity of cotton fabric. It seems, therefore, to be of merit to characterize both the range of sensitive microbes and the dose effects in fabrics, including after multiple wash cycles, to evaluate any real benefit that this preliminary studies implies may exist.

### Acknowledgements

The authors thank Thailand Research Fund and the 90th Anniversary of Chulalongkorn University Fund (Ratchadaphiseksomphot Endowment Fund) for financial support. In addition, Dr. Robert Butcher (PCU, Faculty of Science, Chulalongkorn University) for English corrections and suggestions.

### References

- Chen, C. Z., Beck-Tan, N. C., Dhurjati, P., Dyk, T. K., LaRossa, R. A., & Cooper, S. L. (2000). Quaternary ammonium functionalized poly(propylene imine) dendrimers as effective antimicrobials: Structure–activity studies. *Biomacromolecules*, 1, 473–480.
- Kean, T., Roth, S., & Thanou, M. (2005). Trimethylated chitosans as non-viral gene delivery vectors: Cytotoxicity and transfection efficiency. *Journal of Controlled Release*, 103, 643–653.
- Kim, T. H., Jiang, H. L., Jere, D., Park, I. K., Cho, M. H., Hah, J. W., et al. (2007). Chemical modification of chitosan as gene carrier in vitro and in vivo. *Progress in Polymer Science*, 32, 726–753.
- Lim, S. H., & Hudson, S. M. (2004). Synthesis and antimicrobial activity of a water soluble chitosan derivative with a fiber reactive group. *Carbohydrate Research*, 339, 313–319.
- Majoros, I. J., Williams, C. R., & Baker, J. R. (2008). Current dendrimer applications in cancer diagnosis and therapy. *Current Topics in Medicinal Chemistry*, 8, 1165–1179.
- Marty, J. D., Martinez-Aripe, E., Mingotaud, A. F., & Mingotaud, C. (2008). Hyperbranched polyamidoamine as stabilizer for catalytically active nanoparticles in water. *Journal of Colloid and Interface Science*, 326, 51–54.
- Punyacharoennon, P., & Srikulkit, K. (2008). Preparation of hyperbranched polyamidoamine polymer ultrafine silica hybrid composite. *Journal of Applied Polymer Science*, 109, 3230–3237.
- SayedSweet, Y., Hedstrand, D. M., Spider, R., & Tomalia, D. A. (1997). Hydrophobically modified poly(amidoamine) (PAMAM) dendrimers: Their properties at the air–water interface and use as nanoscopic container molecules. *Journal of Material Chemistry*, 7, 1199–1205.
- Srisuk, S., & Srikulkit, K. (2008). Properties evaluation of sodium nitrite treated chitosan-cotton fabric. *Journal of Metals, Materials and Minerals*, 18, 41–45.
- Tomalia, D. A., Baker, H., Dewald, D. R., Hall, M., Kallos, G., Martin, S., et al. (1985). A new class of polymers: Starburst dendritic macromolecules. *Polymer Journal*, 17, 117–132.
- Tsubokawa, N., & Takayama, T. (2000). Surface modification of chitosan powder by grafting of 'dendrimer like' hyperbranched polymer onto the surface. *Reactive & Functional Polymers*, 43, 341–350.
- Vogtle, F., Gestermann, S., Hesse, R., Schwierz, H., & Windisch, B. (2000). Functional dendrimers. *Progress in Polymer Science*, 25, 987–1041.